Influence of interfaces on magnetization reversal and perpendicular magnetic anisotropy of Fe/Tb multilayers

(*Einfluß der Grenzflächen auf Ummagnetisierungsverhalten und senkrechte magnetische Anisotropie von Fe/Tb-Vielfachschichten*)

Dem Fachbereich Physik - Technologie der Universität - Gesamthochschule - Duisburg zur Erlangung des akademischen Grades eines Doktors der Naturwissenschaften (Dr. rer. nat.) vorgelegte Dissertation

von

Wan-Seop Kim

aus

Daegu/Süd-Korea

Referent: Prof. Dr. Wolfgang Kleemann
Korreferent: Prof. Dr. Eberhard F. Wassermann
Tag der mündlichen Prüfung: 25. 11. 1998

Contents

1. Introduction

Mottos like „more Bytes“ and „faster data transfer“ characterize present day’s expectations on mass storage. Such requirements can only partially be fulfilled with commercial magnetic disc recording systems. Magnetic disc systems are working fast as concerned to read out and write data but are not suitable for saving large amounts of data. Contrastingly optic recording procedure allows high data storage-density and contact-free read out of information. However optic driving systems are not efficient with respect to speed of data recording, reading and transfer. The magneto-optic (MO) offers a new possibility to storage of data, where advantages of the both recording systems combine. Thereby laser light reads information from recorded medium and writes data on a special magnetic recording medium. Proper materials used as the MO recording medium have to fullfill many important requirements e. g. perpendicular alignment of spontaneous magnetization to the film plane, i. e. perpendicular magnetic anisotropy (PMA), large Kerr rotation angle and proper Curie temperature, T_C, in the range 400 - 600 K [Hans90]. In particular the magnetic coercivity (stiffness), H_c, of the magnetic thin films should be high at room temperature (RT), but fall to low values at high temperature at about 600 K.

In search of new recording MO materials Chaudhari et al. [Chau73] presented in 1973 thin amorphous alloy (a-alloy) films of transition (TM) and rare earth (RE) metals like Gd_XCo_{1-X} and Gd_XFe_{1-X} which showed PMA at RT. In addition they carried out first reading and writing experiment and demonstrated that these materials are suitable for MO recording medium. Since then thin films composed of TM and RE elements have intensively investigated not only in view of their potential application for MO recording but also in basic research e. g. towards clarification of the origin for the occurrence of PMA in these films.

Sato et al. [Sato84] presented already in 1984 the first MO disc with diameters of 8 and 12´´ and disc drive systems, in order to record data. In the commercial area Sony presented in 1992 its MO mini disc for recording and playing music. The MO disc operates with thin films of amorphous alloy from iron and terbium with a small addition of cobalt. Here one uses the ferrimagnetic properties of TM and heavy RE elements, where the magnetic moments of heavy RE elements couple antiferromagnetically with the TM moments. Owing to the different temperature dependencies of both sublattice magnetizations a compensation

temperature, T_{comp}, is encountered, where the total magnetization vanishes. At T_{comp} the coercive field H_c is very large, because H_c is inversely proportional to total magnetization. Thereby the recorded information is stable against external magnetic fields. In addition, formation of subdomains by demagnetizing stray fields is suppressed. The important properties for the MO medium, PMA, H_c and T_{comp}, can readily be controlled by a proper choice of elements and their composition. T_C can also easily be controlled by small amounts of cobalt [Dava93].

PMA was also observed in TM/RE multilayers (MLs) [Mori85], which offer better magnetic and magneto-optic properties, e. g. increase of the Kerr rotation, improvement of long-time stability [Kryd85], strong PMA and increasing of magnetization [Sato87a].

In spite of the intensive studies of both TM-RE alloy films and TM/RE multilayers [Shan90, Mibu93] the origin for the occurrence of the PMA is not yet well understood. Many models were proposed including e. g. pair anisotropy [Gamb78, Harr92, Bech97], single ion anisotropy [Sato85, Suzu87, Shan90], growth-induced anisotropy [Leam78, Shin87, Hell92], strain-induced anisotropy [Taka79, Chen89, Huan90], atomic bonding-anisotropy [Egam87, Yan91] and anisotropy by dipolar coupling [Carg78, Mizo79, Fu91] for TM-RE alloys.

Since Fe/Tb multilayers show strong PMA even at RT, where bulk Tb is far from being magnetically ordered, Sato [Sato86] proposed anisotropic distributions of Fe-Tb pairs as a source of the PMA. It is assumed that they preferentially orient perpendicular to the sample plane. Shan et al. [Shan90] combined the pair model with single-ion anisotropy model including non-vanishing orbital moments. Their model is based on the formation of alloys at the Fe/Tb interfaces. Unfortunately this model can only be applied to thin a-TM/RE MLs. Wang et al. [Wang91 - 93] modified the model in order to describe the PMA of MLs with thick single layers. They introduced local crystal fields and strong antiferromagnetic coupling between Fe and Tb magnetic moments and explained temperature dependence of the average canting angle of the crystalline Fe (α-Fe) determined by conversion electron Mössbauer spectroscopy (CEMS) measurements.

Recently, in-situ CEMS measurements on Fe/Tb bilayers, being either Fe-on-Tb (bottom interface) or Tb-on-Fe (top interface), revealed that the top interface primarily induces the

PMA of the α-Fe at low temperature [Scho94a]. Inspecting probe layers of ^{57}Fe with a thickness of about 0.5 nm, sharp interfaces of bcc Fe (α-Fe) are encountered at the top interfaces, whereas they are rough and amorphous at the bottom interfaces [Tapp94]. As a consequence of the different atomic radii and surface energies of Fe and Tb, respectively, the structures of the interfaces are quite different. It is also well-known that the preparation conditions strongly influence the magnetic and crystallographic structures [Malm82]. In particular the layer growth temperature crucially determines the extension of the interfaces [Cher91], their structures and magnetic properties [Dufo91, Rich96a].

The present treatise has been performed within the framework of Sonderforschungsbereich 166 of the Deutsche Forschungsgemeinschaft under the project title „Magnetic and magneto-optic properties of RE-TM thin films and multilayers“. It was aimed at assembling a high-field magneto-optic Kerr (MOKE) spectrometer for operation in ultra-high vacuum (UHV) and investigating the MOKE and magnetic properties of magnetic multilayers composed of transition and rare earth metals. In addition to MOKE spectrometry, SQUID and torque magnetometry supplemented by CEMS are performed. Emphasis has been put on investigating the influence of the interfaces on the magnetization reversal and the origin of perpendicular magnetic anisotropy (PMA) in the system iron/terbium (Fe/Tb), which has a high technological potential for use as a high-density perpendicular magneto-optic recording material.

2. Generalities

In this Chapter different magnetic anisotropies and their physical origins will briefly be reviewed in order to finally understand the PMA of thin TM/RE MLs. Subsequently, the magnetization reversal process based on the coherent rotation model of Stoner and Wohlfarth [Ston48] will be discussed in order to understand hysteresis cycles measured by MOKE and SQUID magnetization.

2.1. Magnetic anisotropy

The phenomenological description of magnetic anisotropy is based on the dependence of the internal energy on the direction of spontaneous magnetization [Chik64]. In this section some main sources of anisotropy will briefly be dealt. We restrict ourselves to those being most important for thin films and MLs and associated with our experiments. Apart from the intrinsic magnetocrystalline and pair anisotropies, extrinsic sources due to the shape and the surfaces of the sample will be discussed.

2.1.1. Magnetocrystalline anisotropy

The free energy density of a crystal is dependent upon the direction of magnetization referring to the crystal axes [Chik64]. It is closely associated with the crystal structure of the system via spin-orbit coupling [Cull72]. For cubic crystals such as α-Fe and Ni the anisotropy energy can be expressed in terms of the direction cosines, α_1, α_2 and α_3, of the spontaneous magnetization $\mathbf{M}_s$ with respect to the three cubic axes. The anisotropy energy density can be expanded into a polynomial series in the α_i. Owing to the high symmetry of the cubic crystal there are many equivalent directions in which the anisotropy energy has the same value. Thus those terms which include odd power of the α_i must vanish because a change in sign of any of the α_i should bring the magnetization vector to a direction which is equivalent to the original direction. Under consideration terms up to the sixth order one obtains the following expression by using the identity $\alpha_1^2 + \alpha_2^2 + \alpha_3^2 = 1$ [Chik64]

$$E_a = K_0 + K_1(\alpha_1^2\alpha_2^2 + \alpha_2^2\alpha_3^2 + \alpha_3^2\alpha_1^2) + K_2\alpha_1^2\alpha_2^2\alpha_3^2 + \cdots \quad (2.\ 1)$$

with material-specific anisotropy energy density constants K_0, K_1 and K_2.

A corresponding consideration can be applied to hexagonal crystals. The anisotropy energy density can be expressed analogously to Eq. (2. 1) as follows [Birs66]

$$E_a = K_1 \sin^2\theta + K_2 \sin^4\theta + \cdots, \quad (2.\ 2)$$

where θ is the angle between the direction of $\mathbf{M}_s$ and the c axis of the crystal. In the case $K_1 > 0$ and $K_2 > 0$ the hexagonal c axis is the direction of easy axis and the anisotropy energy density in the basal plane ($\theta = \pi/2$) is maximum along all directions. Higher order terms may break this planar isotropy.

The anisotropy constants influence the magnetization reversal process of homogeneously magnetized materials. The shape of the hysteresis cycles strongly depends not only upon magnitude of the anisotropy constants but also on their signs [Oliv97]. Generally the second order constant K_2 (e. g. $\pm 5 \cdot 10^3 J/m^3$ for α-Fe) is considerably smaller than K_1 ($4.8 \cdot 10^4 J/m^3$) [Chik64, Pear79] so that it is sufficient in many cases to take into consideration only the first term (K_1 or second order of direction cosine). Thus the anisotropy energy density E_a is expressed as

$$E_a = K_u \sin^2\theta \quad (2.\ 3)$$

with the uniaxial anisotropy energy density constant K_u. For positive K_u the spontaneous magnetization lies perpendicular to layer plane whereas it lies in the sample plane for negative K_u.

2. 1. 2. Surface anisotropy

It was first pointed out by Néel [Néel54] that the atoms located near at surface have a different environment as compared to bulk ones. Hence, they experience symmetry breaking and give additional contributions to the magnetic anisotropy. This surface anisotropy density E_s can be expressed as

$$E_s = \frac{2K_s}{t}\sin^2\theta \qquad (2.\ 4)$$

with the surface anisotropy energy density constant K_s and the thickness t of the magnetic layer. θ is the angle between the magnetization direction and the normal to the surface. The factor 2 occurs due to the two surfaces of a magnetic layer. Generally the both surface anisotropy constants, K_{st} (top) and K_{sb} (bottom), are equated for sake of simplicity. However, in the case of Fe/Tb MLs it is well-known that the structure of both interfaces, top and bottom, of the individual Fe layers behave differently (see above) [Scho94a, Tapp94, Rich96a]. Here Eq. (2. 4) should be rewritten as

$$E_s = \frac{K_{st} + K_{sb}}{t}\sin^2\theta. \qquad (2.\ 5)$$

2. 1. 3. Shape anisotropy

The magnetic anisotropy of thin layers is strongly influenced by their geometry. At the surfaces of homogeneously magnetized sample magnetic poles are forming. A demagnetizing field $\mathbf{H}_d$ in the inside of the sample is produced by the potential of these free poles. $\mathbf{H}_d$ is oriented antiparallel with respect to the magnetization **M** of the sample (see Fig. 2.1) and

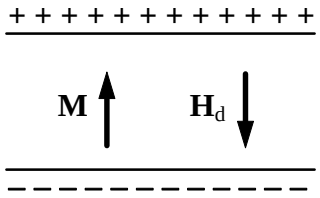

*Fig. 2.1: Demagnetizing field $\boldsymbol{H}_d$ due to the Magnetization **M** normal to the surface of a thin layer*

can be expressed as

$$\boldsymbol{H}_{\mathrm{d}} = -\tilde{\boldsymbol{N}}\,\boldsymbol{M}. \tag{2. 6}$$

The shape anisotropy energy density E_d can be expressed as

$$E_d = -\frac{\mu_0}{2V}\int_V \mathbf{H}_d \cdot \mathbf{M} dV. \tag{2. 7}$$

The demagnetizing tensor $\tilde{N}$ is dependent upon the distribution of the magnetic poles and thus upon the geometry of the sample. It can exactly be calculated only for special sample geometries, e. g. for rotational ellipsoids [Cull72, Chik64]. A thin layer can approximately be considered as a flat disc, where the lateral dimension is much larger than the thickness of the layer. In this case the demagnetizing tensor can be transformed onto the principal axes of an ellipsoid (see e. g. [Cull72]) and may be read as demagnetizing factors N. It vanishes in the plane, $N_{\parallel} = 0$, and maximizes perpendicular to the sample plane, $N_{\perp} = 1$, [Chik64]. Generally, Eq. (2. 7) can be written in the thin layer limit as

$$E_d = -\frac{\mu_0}{2}(N_{\perp} - N_{||}) M_S^2 \sin^2\theta, \tag{2. 8}$$

where θ the angle between the magnetization direction $\mathbf{M}_s$ and the sample normal. According to Eq. (2. 8) E_d of thin layers is minimal in the sample plane so that $\mathbf{H}_d$ favors the spontaneous magnetization to lie in the sample plane.

2.1.4. Pair anisotropy

The pair anisotropy model proposed by Van Vleck [Vlec37] describes the contribution to magnetic anisotropy energy due to pseudodipolar interaction of all atomic pairs. The most important interaction between the atomic moments is the exchange interaction. But this energy is dependent only on the angle between neighboring atomic moments, independently of their orientation relative to their bond direction, and so it does not give rise to anisotropy. In

order to explain magnetic anisotropy we assume that the pair energy is dependent on the direction of the magnetic moment **m**, φ, as measured from the bond direction (see Fig. 2.2). The interaction energy w of a atomic pair at distance r can be expressed by an expansion into Legendre polynomials neglecting higher order terms [Chik64]

$$w(\cos\varphi) = g + l(\cos^2\varphi - \frac{1}{3}) + q(\cos^4\varphi - \tfrac{6}{7}\cos^2\varphi + \tfrac{3}{35}) + \cdots. \qquad (2.\ 9)$$

The first term in Eq. (2. 9) is independent of φ. Hence, the exchange energy is to be included in this term. The second term is called the dipole-dipole interaction term and the third term the quadrupolar interaction etc. If the pair energy were exclusively due to magnetic dipolar interaction the estimated value is in most cases 10^2 - 10^3 times larger than that of calculated ones [Chik64]. The origin of this strong deviation is believed to be a combined effect of spin-orbit interaction and exchange or Coulomb interaction between neighboring orbits [Chik64]. These types of interactions are the anisotropic exchange and are called pseudodipolar, pseudo-quadrupolar etc. interactions.

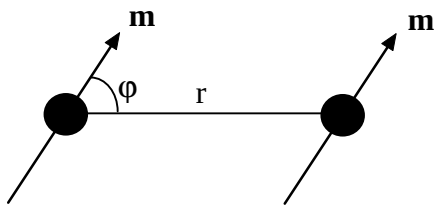

*Fig. 2.2: A par of magnetic atoms with moments **m** in distance r; φ is the angle between magnetic moments and the binding line*

An interaction like that described by Eq. (2. 9) between the atomic moments gives rise to magnetic anisotropy. This magnetic anisotropy energy can be obtained by adding up all the atomic pair energies. If we let α_i, i = 1, 2 and 3, denote the direction cosines of the magnetization, cosφ in Eq. (2. 9) can be replaced by α_i for those atom pairs whose bond direction is parallel to the i axis. Thus the magnetic anisotropy energy can be expressed by [Chik64]

$$E_{ap} = \sum_i w_i = -2Nq(\alpha_1^2\alpha_2^2 + \alpha_2^2\alpha_3^2 + \alpha_3^2\alpha_1^2) + const., \qquad (2.\ 10)$$

where i is an index attached to each of the atom pairs and N is the number of atoms included in the unit volume. Comparing this with Eq. (2. 1) it is easy to find the relation $K_1 = -2Nq$ for a simple cubic lattice [Chik64].

It should be noted here that the dipolar term of Eq. (2. 9) does not contribute to the interaction energy because the contributions of different binding directions are averaged [Chik64]. Contrastingly van Vleck [Vlec37] pointed out that the dipole-dipole interaction contributes to anisotropy energy because the perfect parallel arrangement of spins are disturbed by dipolar interaction. The dipolar interaction of crystal with lower symmetry than cubic system, e. g. hexagonal system, contributes to anisotropy [Chik64].

The pair anisotropy was proposed as source of the PMA for a-alloys composed of TM and RE elements, e. g. GdCo [Gamb78] and FeTb thin alloy films [Dove85]. The explanation of the authors meets the conditions of samples prepared by sputtering techniques owing to the different stability of various RE-RE, RE-TM and TM-TM pairs during the sputter process.

A direct proof of anisotropic distribution of atom pairs is difficult. Recently this was investigated by using „extended x-ray absorption fine structure“ (EXAFS) measurements on thick a-FeTb alloys [Robi89, Harr92]. The studies showed that the pairs of like atoms and their axes preferentially lie in the sample plane whereas pairs of different atoms are oriented perpendicular to the sample plane. Wang et al. [Wang90] showed that a 0.4% excess of anisotropic atom pairs is enough to explain the anisotropy energy observed on a-TM-RE alloys. In particular such excess in anisotropic atom pairs can readily be realized with the help of MLs. This was the reason why Sato [Sato86] prepared MLs from TM and RE elements.

Unfortunately this model does not completely explain the PMA observed. MLs from Fe and Gd, and Y, respectively, show no PMA in contrast with those from Fe and Tb [Mibu93]. This means that the anisotropic distribution of atom pairs alone is not sufficient to induce the PMA of the TM/RE MLs. Besides it is also not clear how microscopic short-range order, local TM-RE atom pairs, leads to macroscopic PMA in thick TM-RE alloys, where the total pair anisotropy should be averaged and should be cancelled out.

2.1.5. Single-ion anisotropy

The single-ion anisotropy is caused by electrostatic interaction of the 4f electron of the RE-atoms with the local electric field due to the surrounding atoms. The non-spherical charge distribution of the 4f electrons caused by their anisotropic structure (see below) leads to spatial alignment of 4f orbital and its angular momentum. Hence, the alignment of the total magnetic moments occurs due to spin-orbit coupling [Sato87b, Shan90]. The anisotropy of the crystal fields has been attributed either to the formation of atom pairs in the interfaces [Gamb78] or to strain and tension, respectively, during sample preparation [Taka79, Yasu81].

Sato et al. [Sato85] studied the PMA of a-GdCo alloys after addition of small amounts of RE elements, Tb, Dy, Ho or Er, by using torque magnetometry. This study showed that the change of PMA due to the RE elements agrees very well with the contribution to the anisotropy energy calculated on the basis of the single-ion model adapted to the respective RE element.

In the MLs composed of RE and TM elements structural anisotropy always happens due to the formation of atom pairs at the interfaces. However TM/RE MLs fulfilling the same conditions, e. g. the same single layer thicknesses, do not always show PMA, e. g. Fe/Er, Fe/Gd, Fe/Y, neither at low temperature T = 4.2 nor at 300 K [Mibu93].

2.2. Magnetization reversal process

The magnetization reversal behavior of a homogeneously magnetized elongated fine particle with uniaxial anisotropy constant density is described by the Stoner-Wohlfarth (SW) model [Ston48]. This model has been adapted and applied to the magnetization reversal in thin films. Consider a uniform thin film having the spontaneous magnetization M_s and a uniaxial anisotropy constant K_u. Assuming coherent magnetization processes, the total energy density in an applied field **H** including of the crystalline, shape and surface anisotropy energies and the Zeeman energy caused by the applied field is given by

$$E_{tot}/V = K_u \sin^2\theta - \frac{1}{2}\mu_0 M_s^2 \sin^2\theta + \frac{2K_s}{t}\sin^2\theta - \mu_0 H M_s \cos(\varphi - \theta), \qquad (2.\ 11)$$

where V is the volume and t the thickness. The angles φ and θ are defined in Fig. 2.3.

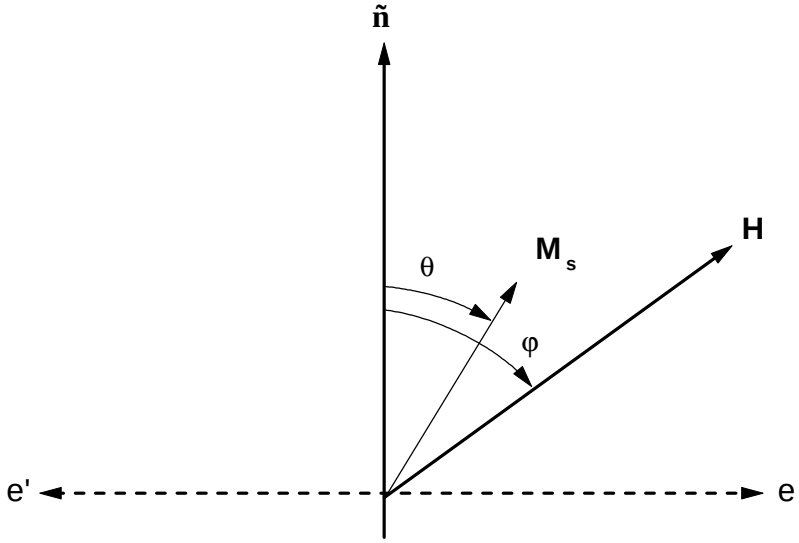

Fig. 2.3: Illustration of geometry referring to the Stoner-Wohlfarth model, Eq. (2. 9), where ***H*** *= applied field,* $\mathbf{M}_s$ *= spontaneous magnetization,* $\tilde{\mathbf{n}}$ *= layer normal,* $\theta = \sphericalangle(\tilde{\mathbf{n}}, \mathbf{M}_s)$, $\varphi = \sphericalangle(\tilde{\mathbf{n}}, \mathbf{H})$ *and ee' = cross section of the layer*

The first 3 terms show the same angular dependence so that they can be contracted into an effective anisotropy constant $K_{eff} = K_u - \frac{1}{2}\mu_0 M_s^2 + \frac{2K_s}{t}$. Then Eq. (2. 11) can be rewritten

$$E_{tot}/V = K_{eff} \sin^2\theta - \mu_0 H M_s \cos(\varphi - \theta). \qquad (2.\ 12)$$

The alignment of the spontaneous magnetization depends on the sign of K_{eff}. If $K_{eff} > 0$, then $\mathbf{M}_s$ orients parallel to $\tilde{\mathbf{n}}$, whereas $\mathbf{M}_s$ lies in the plane ee' when $K_{eff} < 0$.

The direction of $\mathbf{M}_s$ spontaneously aligned in the applied field is determined by minimization of the total energy density, $\partial E_{tot}/\partial\theta = 0$:

$$\frac{1}{V}\frac{\partial E_{tot}}{\partial \theta} = K_{eff}\ \sin 2\theta - \mu_0 H M_s \sin(\varphi - \theta) = 0 \qquad (2.\ 13)$$

$$\Rightarrow\ \sin\theta(2K_{eff}\ \cos\theta - \mu_0 H M_s) = 0 \qquad (2.\ 14)$$

$$\Rightarrow\ \cos\theta = \frac{H}{H_k}, \qquad (2.\ 15)$$

with **H** || **ñ** (φ = 0) and $H_k = \frac{2K_{eff}}{\mu_0 M_s}$.

The non-trivial solution of Eq. (2. 14) yields the magnetization curves by inserting Eq. (2. 15) into the field-parallel component, $M(H) = M_S\cos\theta$, as shown in Fig. 2.4. More details are to find in [Mans95].

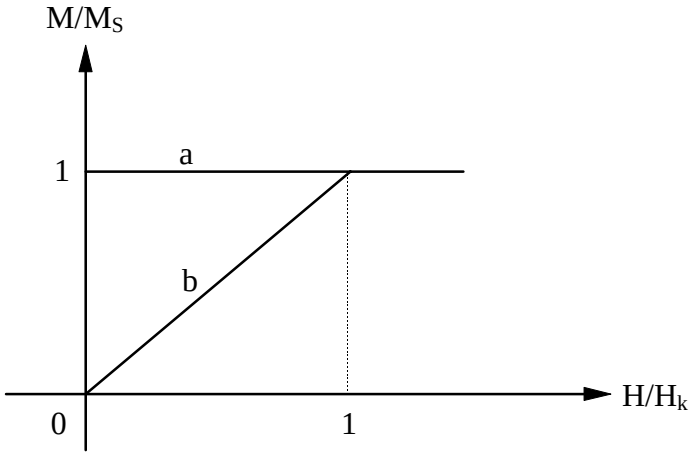

Fig. 2.4: Magnetization curves (first quadrant) of an ideal SW particle; curve a: applied field parallel to the easy axis(e. a.), curve b: applied field perpendicular to the e. a.

The saturation field strength H_s can easily be determined from Eq. (2. 15), since $\cos\theta = 1$ at saturation, and is given by

$$H_s = H_k = \frac{2K_{eff}}{\mu_0 M_s}. \qquad (2.\ 16)$$

This relation allows us to determine either K_{eff} at known M_s or vice versa from magnetization or Kerr hysteresis cycles. Generally a quantitative determination of M_s from Kerr hysteresis loops is not possible in the absence of the proportionality constant between Kerr intensity and

magnetization. Besides, the Kerr intensity is strongly dependent upon the wavelengths used. In the case of in-plane magnetization one can readily determine K_{eff} from the Kerr loops by measuring H_s and inserting M_s into Eq. (2. 16).

In real systems the magnetization curves deviate from the ideal curves as shown in Fig. 2.4, where the magnetization reversal does not happen through homogeneous rotation of magnetic moments. In many cases the single domain decays into a multidomain state through nucleation, whereby the stray field is minimized. The occurrence of regions with different orientations separated by domain walls results in magnetization reversal processes, which starts at lower field than calculated according to the SW model. In addition, it saturates at a larger field value than the calculated ones owing to the stray fields of the domains, which are oriented antiparallel to the applied field and partially compensate the external field [Vale94, Nowa97].